MEKATRONIKA
JOURNAL OF MECHATRONICS AND INTELLIGENT MANUFACTURING
E-ISSN: 2637-0883
VOLUME 7, ISSUE 2, JULY 2025, 124 - 133
DOI: https://doi.org/10.15282/mekatronika.v7i2.11321

RESEARCH ARTICLE

Machine Learning-Based Change Detection for Land Use Land Cover in Malaysia

Muhammad Fareed Mohd Noor[1], Noor Zarikh Khuzaimi Rahmat[2], Nur Azam Abdullah[2], Azhar Mohd Ibrahim[1], Suaib Al Mahmud[1], Muhammad Imran Mardzuki[1]*

[1]Department of Mechatronics Engineering, International Islamic University Malaysia, Jalan Gombak, 53100 Kuala Lumpur, Malaysia
[2]Department of Mechanical and Aerospace Engineering, International Islamic University Malaysia Jalan Gombak, 53100 Kuala Lumpur, Malaysia

ABSTRACT - Remote sensing has gained widespread attention due to its applications and technological advancements. This study aims to explore the use of remote sensing for change detection for land use land cover (LULC). The study begins by focusing on pre-processing, including radiometric, geometric, and atmospheric correction as well as image enhancement to produce quality images for further classification analysis. Two classification methods were explored: supervised and unsupervised. For supervised classification, Support Vector Machine (SVM), Classification and Regression Tree (CART), and Random Forest classifiers were tested. After thorough evaluation, it was determined that the Random Forest algorithm was the optimal choice, yielding a training accuracy of 99.6% and a test accuracy of 80% for LULC classification. For unsupervised classification, a cluster classifier was used. Change detection is then conducted through image subtraction of two different timelines. Supervised classification of LULC images resulted in a total change of 94.74 km² across three locations: Wang Kelian, Sungai Golok and Pengerang while unsupervised classification resulted in change of 23.56 km² for Lahad Datu and 20.51 km² for Sungai Golok.

ARTICLE HISTORY
Received : 23rd Sept. 2024
Revised : 10th Feb. 2025
Accepted : 11th July 2025
Published : 30th July 2025

KEYWORDS
Remote sensing
Satellite imagery
Land cover
Machine learning
Change detection

1. INTRODUCTION

Remote sensing involves acquiring information about Earth's surface by detecting reflected or emitted electromagnetic radiation (EMR). It functions through passive systems that utilize natural energy and active systems that emit their own energy and record reflections. Satellite sensors act as intermediaries, converting EMR, affected by atmospheric interactions, into electronic signals known as channels [1]. Despite its wide-ranging applications, the full integration of remote sensing into decision-making processes remains limited. This underutilization is often due to the rapid pace of technological advancement, which outpaces adoption. Nonetheless, remote sensing has shown clear advantages in vegetation monitoring, land mapping, and environmental assessment. In Malaysia, although ongoing research explores these areas, broader application and deeper analysis, particularly in land use/land cover (LULC) change detection remain areas for improvement [2]. Remote sensing technologies can be categorized into analog and digital systems [3]. Analog approaches record EMR on film, while digital systems rely on satellite-based sensors. LandSat, for example, uses both multispectral and hyperspectral sensors. Multispectral sensors capture broad spectral bands with high spatial but low spectral resolution. Traditional filter wheel systems are often bulky and power intensive. To overcome these limitations, the High Precision Telescope (HPT) with a Liquid Crystal Tunable Filter (LCTF) has been introduced, improving efficiency and spectral coverage while reducing hardware constraints [4]. Hyperspectral sensors, on the other hand, collect data across hundreds of narrow spectral bands, providing high spectral resolution but typically lower spatial resolution. These sensors are increasingly used in fields such as agriculture and medical diagnostics [5]. However, they face performance trade-offs due to energy limitations and the need to optimize the signal-to-noise ratio (SNR). A comparative study examined several hyperspectral and multispectral sensors on unmanned aerial systems (UAS) for soil organic carbon mapping [6]. The sensor characteristics are detailed in Table 1.

Table 1. The spectral resolution of the sensors used

Instrument	Type	Wavelength Range (nm)	Output Resolution (nm)	Spectral Windows (nm)
ASD	Hyperspectral	350-2500	1	-
STS-VIS	Hyperspectral	350-800	0.45	-
STS-NIR	Hyperspectral	650-1100	0.45	-
Sequioia	Multispectral	-	-	550±20, 660±20, 735±5, 790±20, 480±5, 550±5
Mini-MCA6	Multispectral	-	-	670±5, 780±5, 880±5, 1000±5

***CORRESPONDING AUTHOR | Muhammad Imran Mardzuki** | ✉ Imranmardzuki881@gmail.com

The study suggested using visible and near-infrared (VIS-NIR) for precise estimation of spatially distributed Space Operation Complex (SOC) data. Multispectral and hyperspectral sensors can be used to measure soil organic carbon on bare soils with acceptable precision and at a significantly greater spatial as well as temporal resolution than current methods. Various studies were conducted to implement remote sensing in various fields. One is where they assessed the possibilities and limitations of remote sensing techniques as a tool for data monitoring at the Wadden sea and to provide information on developments of channels and gullies, morphology, and sediment characteristics [7]. In this study, they aimed to ensure that the collected data is not influenced by clouds and weather, and this is the reason why they were using ERS satellite in this study which provided data in black and white. The findings of this study suggest that throughout each historical satellite mission the data is limited to around 4 images per year. This causes trend and other analysis of sediments to be limited.

Remote sensing is a method that enables the analysis of map properties and helps convert data into useful information such as land cover maps. In a study conducted in Kelantan, Malaysia, information was obtained from land cover mapping, which provided details on specific features of the map such as built areas, cleared land, forests, and oil palm [8]. This process translates and filters raw data into a format that is easily understood by people and enables the transformation of normal picture maps into valuable information. The land cover map of Kelantan state is shown in Figure 1. The unique chemical composition of each object on the ground results in different reflections of electromagnetic radiation. This gives each object a unique spectral signature that can be used to distinguish it from other objects based on the differences in reflected electromagnetic radiation at different wavelengths. Spectral signatures provide qualitative and quantitative information about image classification. NASA has provided a graphical chart showing the average spectral reflectance curves for three basic earth features: healthy green vegetation, dry bare soil, and clear lake water. These curves demonstrate key features of spectral reflectance.

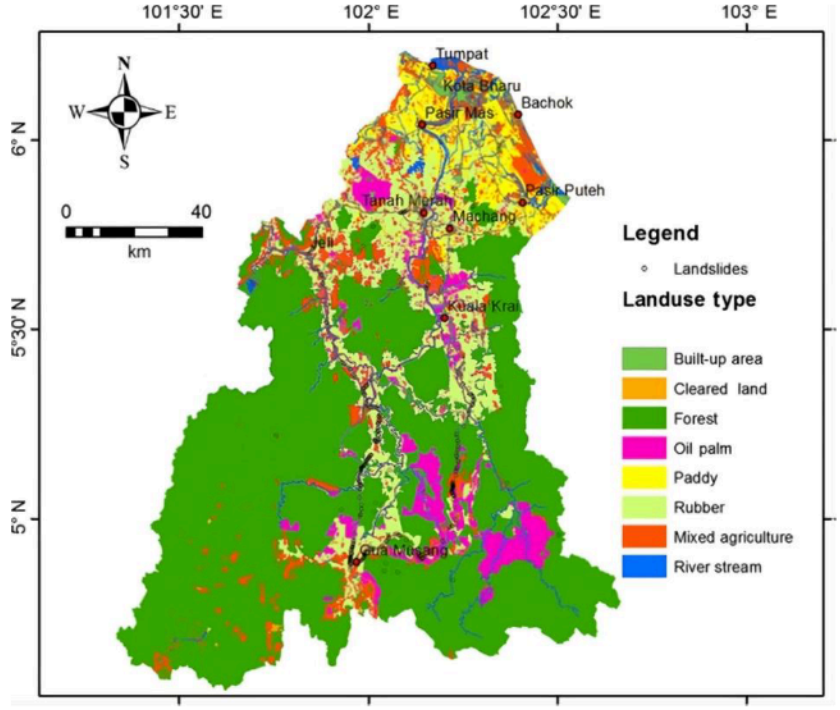

Figure 1. Land cover map of the Kelantan state

Change detection is the practice of finding differences in the condition of an object or phenomenon by watching it at different times [9]. Change detection focuses on when, where and what kind of change occurred, how much has changed, and what are the cycles and trends of the changes. One of the methods is classification. This approach makes the use of categorized images of historical data as training data. Its' benefits and values include the production of change matrices and the elimination of outside variables. It is essential to choose an acceptable sample data set. The next category is an advanced model which this method uses to turn image reflectance value into physical parameters, which are capable of extracting information more efficiently than spectral signatures but take longer time and are more challenging [10]. The main aims of this study are firstly to produce high-quality satellite imagery through the effective implementation of pre-processing, image correction and image enhancement techniques, secondly to establish supervised and unsupervised classification models that are capable of classifying land cover, and finally to demonstrate the performance evaluation of the classification and to detect potential changes of land use land cover (LULC).

2. METHODOLOGY

As illustrated in Figure 2, the study begins with pre-processing of satellite imagery datasets. This includes image enhancement like improving the visual quality if the satellite imagery and image correction like radiometric, geometric, and atmospheric correction, which reduce errors in the data. Next the study continues with a discussion on machine learning and image classification, explaining why a specific classifier is suitable for LULC classification. The study employs supervised classification and unsupervised classification approach, which clusters similar characteristics into groups using only unlabelled data, to uncover patterns. The method for unsupervised classification is commonly used in situations where labelling would be cost-prohibitive or unnecessary [11]. Additionally, how change detection results using the classification results is obtained are discussed.

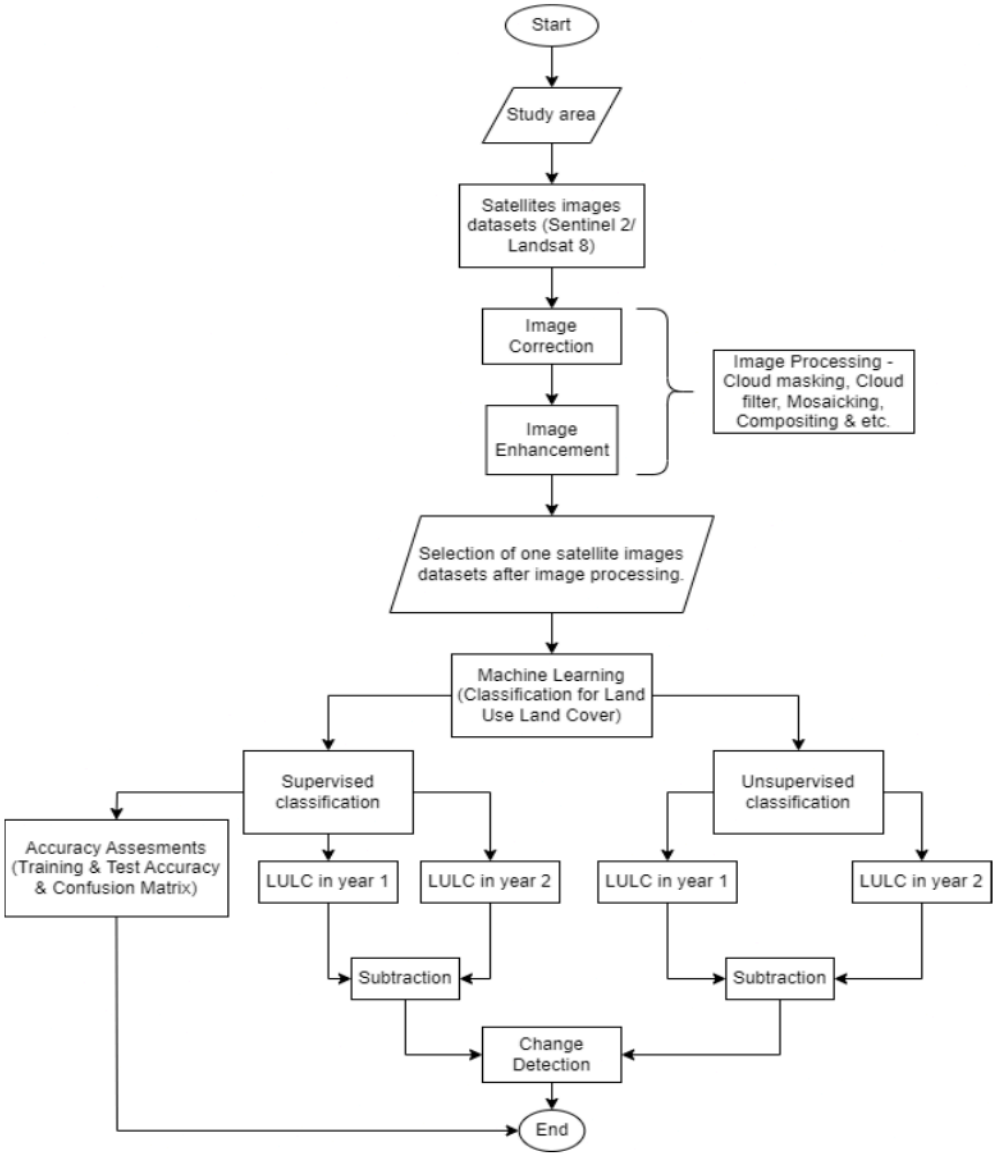

Figure 2. Flowchart of research methodology

2.1 Image Processing

In general, the pre-processing phase is designed to improve the quality of an image as a foundation for subsequent analysis. It is crucial to properly analyse satellite images. The datasets we have selected are raw data from study area that contain several artifacts and errors which need to be corrected to reduce error and improve data quality and accuracy. These errors can be divided into two categories: geometric errors and radiometric errors.

Geometric errors occur when an images' coordinates differ from those expected under ideal conditions. Examples of this include slant range projection, foreshortening, layover, and shadowing [9]. Radiometric errors, on the other hand, occur when the brightness values recorded in an image do not accurately reflect the reflectivity or density of the object being digitized. Examples of radiometric errors include the spreading loss effect, non-uniform antenna pattern, potential gain variations, saturation, and speckle noise.

2.2 Image Correction and Image Enhancements

This is part where the image correction and image enhancements are applied. For image correction in remote sensing there are three types of image corrections which are radiometric correction, geometric correction, and atmospheric correction. Image correction and enhancements are applied in remote sensing to remove or correct any errors or distortions in the acquired images that could negatively impact the interpretation of the data. The main sources of errors in remote sensing images are atmospheric distortion, sensor characteristics, and geometric distortion. Image correction is used to remove or minimize these errors.

Radiometric correction is applied to correct errors caused by variations in the sensors' response to the amount of energy it receives. These variations can occur due to changes in the sensors' sensitivity, the angle of the sun, or the presence of clouds or other atmospheric conditions. Geometric correction is applied to correct errors caused by the sensors' position and attitude when acquiring the image, as well as any distortions caused by the sensors' optics. This can include correction for distortions such as perspective and relief displacement, which are caused by the sensor's viewing angle and the terrains' topography. Atmospheric correction is applied to correct errors caused by the presence of gases, particles, and water vapor in the atmosphere that can absorb, scatter, or reflect the energy being detected by the sensor. This can include correction for atmospheric absorption and scattering that can affect the radiometry of the image. Then, image enhancement is applied to improve the visual appearance of the image, to highlight features of interest or improve image contrast which would help in easier interpretation of the image.

2.3 Image Classification

After obtaining an accurate representation of the target surface through image correction and enhancement, the next step is to proceed with image classification utilizing machine learning algorithms. Image classification techniques, based on spectral reflectance, are used to categorize pixels in satellite data for identifying distinct earth features. This method is commonly used to create a LULC map. There are three primary methods used for image classification: supervised classification, unsupervised classification, and object-based image analysis. Each method utilizes a different algorithm to create land cover, but each has its own limitations and may not classify images perfectly. For context, unsupervised classification is a classification process that utilizes computer assistance without a prior knowledge of the specific classification. Object-based image analysis, on the other hand, creates square pixels with a class for each pixel, and these pixels are grouped into representational vector shapes, each with its own size and geometry.

In this study, we focused on using supervised and unsupervised classification. Clustering algorithms are utilized in unsupervised learning models. Clustering analysis employs similarity criteria to group data points that are near each other and separate those that are not [10]. It is a widely used method in market segmentation, pattern recognition, and image processing. One of the most popular and simple clustering algorithms, K-means, can be used to solve both supervised and unsupervised machine learning problems [11]. The algorithm begins with a pre-determined number K, and then assigns each point to the cluster closest to it. Next, the cluster centroid is determined, and each point is re-allocated to the new cluster. The cluster centroids are re-calculated, and the re-assignment process is repeated until the error reaches a certain threshold.

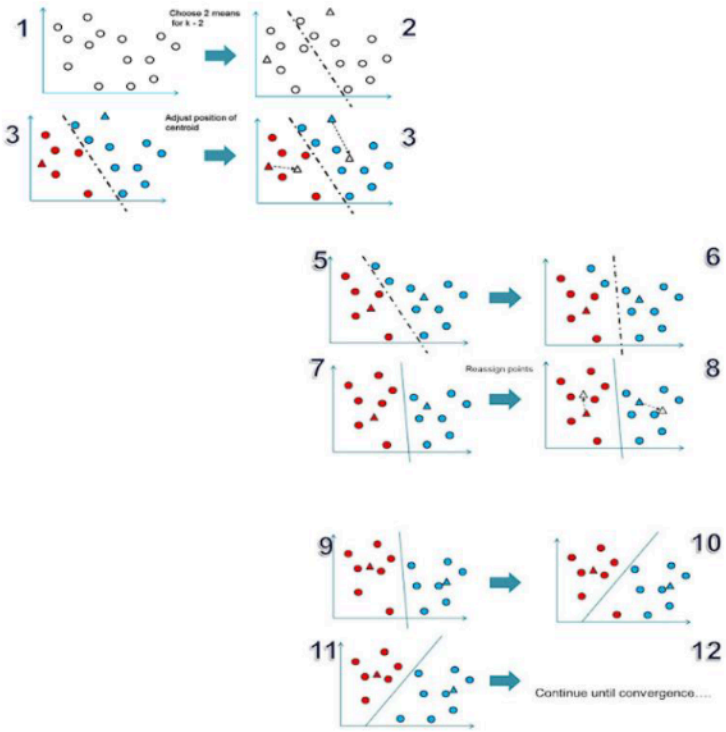

Figure 3. K-means visualization

To perform supervised classification, it is necessary to gather data to select land cover classes as training sites using a visual digitizing approach such as by adding training sites and marking areas such as urban, water, vegetation, or other areas that are represented in the images. The process continues by creating training samples for each land cover class until each class has representative samples. As a result, a signature file is created, containing the spectral information of all training samples.

2.4 Change Detection

Earth observation datasets that are accessible at regular intervals over extended time periods can be used to identify changes on Earths' surface. There are six categories of change detection techniques, each with its' own use and purpose, and among the change detection techniques, the method image differencing is particularly suitable for use with the Google Earth Engine (GEE) platform [12]. Therefore, it is highly recommended for use when conducting analysis for the classification of LULC. To utilize this method, LULC classification was conducted for specific locations at two different points in time. The results of the two classifications were then subtracted from each other to produce the result of the change. By utilizing the specific code available in GEE, this method can yield accurate results.

The change detection approach, which is image differencing, is particularly suitable for detecting urban land cover change and change in forest ecosystems [13]. This method involves subtracting the Digital Number (DN) value of two spatially registered images taken at different times, pixel by pixel and band by band. If a difference in DN value is observed, it indicates a change in the area. However, if no difference in DN value is observed, it does not necessarily indicate that no change has occurred on the earth's surface [14]. This is due to the fact that exact image registration and ideal radiometric conditions are rarely achieved for images captured at different dates.

3. RESULTS AND DISCUSSION

3.1 Managing Satellites Imagery

The best platform for this research is GEE. GEE is a cloud-based geospatial analysis tool that allows users to visualize and study satellite imagery of the Earth. It is widely used by scientists, non-profits organizations and governments for remote sensing research, disease outbreak prediction, natural resources management and other applications. The public data archive of GEE includes more than 40 years of historical images and scientific datasets, which are continuously updated and expanded. It comprises of around 40 petabytes of geographical data that can be instantly accessed. In simple terms, GEE allows users to add datasets to their script environment with just a few clicks and lines of code. Users can also upload their own raster or vector data for personal use or sharing. All pre-processing, post-processing, and other tasks can be performed using JavaScript in the Code Editor.

Even though the GEE platform provides a vast collection of satellite datasets, not all of them are appropriate for LULC. For this research, we have evaluated several satellites to obtain the most suitable datasets. The satellites that we have used for this study are Sentinel-2 and Landsat 8. Sentinel-2 is a global wide-swath, high-resolution multispectral imaging mission with a five-day revisit frequency. It provides data that can be used to assess the state of vegetation, soil, and water coverage as well as changes over time. Meanwhile, Landsat 8 Surface Reflectance in GEE provides data on land surface temperature and surface reflectance that has been atmospherically corrected.

Many of the satellite imagery datasets in Earth Engine are stored in ImageCollections. In this research, since we were working with Sentinel-2 and Landsat 8 datasets, we needed to locate the Image Collection IDs in the Earth Engine Data Catalog. Since we decided to use surface reflectance datasets, we used "COPERNICUS/S2" and "LANDSAT/LC08/C02/T1_L2". To view the RGB visual of the raw data, we selected the appropriate band combination and specified the correct minimum and maximum gamma values. The band combinations that we used are 'B4', 'B3', and 'B2'. The figure below illustrates the result of the raw data of Sentinel-2 MSI: MultiSpectral Instrument, Level-1C and USGS Landsat 8 Level 2, Collection 2, Tier 1.

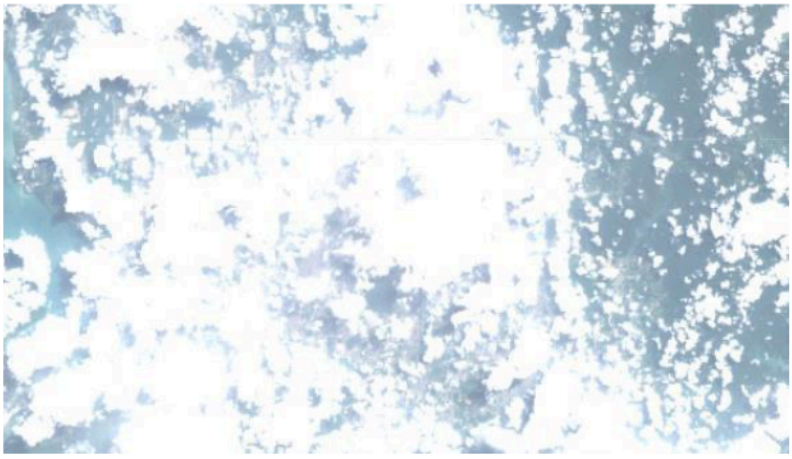

Figure 4. Raw data of Sentinel-2 ("COPERNICUS/S2")

Figure 5. Raw data of Landsat-8 ("LANDSAT/LC08/C02/T1_L2")

As seen from Figure 4 and Figure 5, this collection is not ideal for many applications as it requires a subset of the images. Therefore, we proceeded to perform filtering, compositing, mosaicking, and cloud masking to achieve a better result of the images. The three most common filters in Google Earth Engine are filtering by metadata, filtering by date and filtering by location. The use of metadata filtering is to filter out cloud pixel percentages, while date filtering is to select images within a specific date range, and location filtering is to select a subset of images using a box, a location, or geometry. We clipped the specific locations, filtered out 10% of the cloud pixels, and filtered by date for the year 2020 and 2021. Then, we created a mosaic image with the most recent pixels on top by calling mosaic function and created a median composite image in which each pixel's value equals the median of all stack pixels by calling median function. Lastly, we applied cloud masking to improve product generation and to make the analysis process easy in further supervised classification. The codes used to apply these image processing techniques for Sentinel-2 and Landsat-8 are different. Therefore, we implemented and coded them separately for each image collection. The results of the code applied for the images with a region Wang Kelian can be seen from Figure 6.

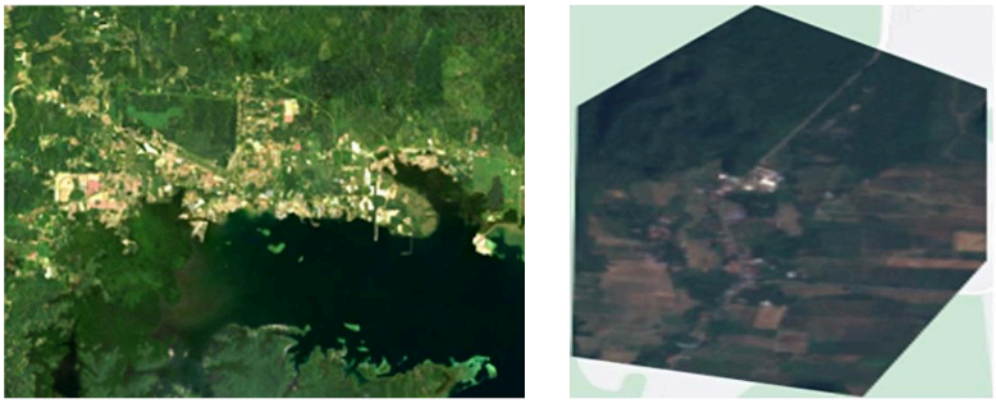

(a) (b)

Figure 6. (a) Result of Landsat-8 after image processing at Lahad Datu; (b) Result of Sentinel-2 after image processing at Wang Kelian

Overall, cloud filtering is a crucial stage in remote sensing as it eliminates clouds and other atmospheric distortions from satellite and aircraft images. The use of several methodologies and data sources in combination can provide accurate and comprehensive cloud filtration, leading to optimal results. It is essential to have high-quality images for the next stage, which involves image classification for Land Use and Land Cover (LULC) using both supervised and unsupervised classification methods.

3.2 Machine Learning

As can be observed from previous figures, the images have been filtered resulting in clearer images. These images serve as training data for supervised and unsupervised classification. To accomplish the unsupervised classification, a clustering method, specifically K-means, has been utilized to determine the land cover before a change detection technique is employed to detect any changes for both locations in 2020 and 2021. K-means was selected due to its simplicity, computational efficiency, and its ability to automatically group pixels based on spectral similarity without requiring any prior knowledge or labelled data [15]. Five different random classes have been assigned without any prior knowledge or training data about the image. The use of random classes in unsupervised classification serves as a benchmark or baseline for comparing the performance of different algorithms or parameters. The ability of the algorithm

to distinguish between different types of land cover or other features in the image can be evaluated by comparing the results of unsupervised classification to the randomly assigned classes. Figure 7 show the image after unsupervised classification has been implemented.

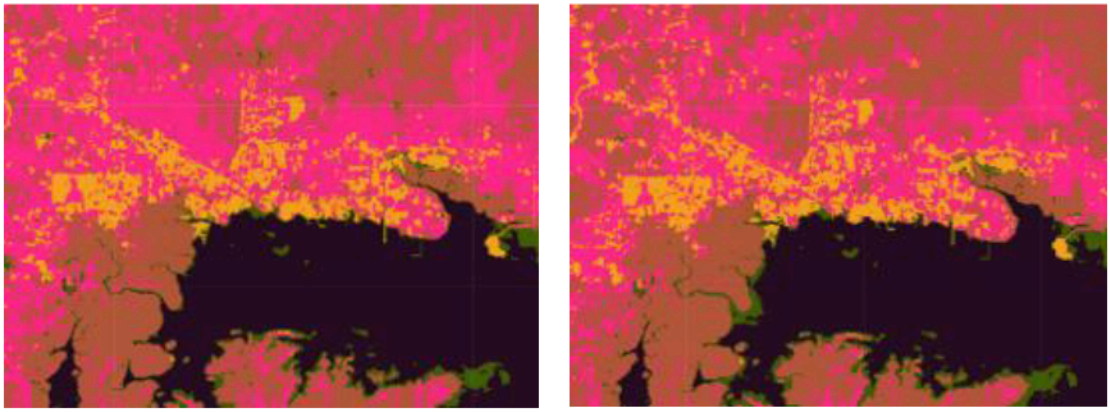

(a) (b)

Figure 7. LULC at Lahad Datu by using K-means for the year (a) 2020 (b) 2021

For supervised classification, the study also categorized it into 5 classes, but specificity is required for supervised classification. This approach does not require any prior training data and may be used to create high-quality classification samples anywhere on the planet. We categorized each source pixel and built four new feature collections with points representing pixels of that class using the code editors' drawing tools. Each feature collection contains a landcover attribute with values of 0, 1, 2, 3, and 4 that indicate whether the collection represents vegetation, road, urban area, bare land, and water. We visually selected the training points using naked eye and placed them onto the map with all these characteristics for the year 2020 and 2021. Each year had 100 points for each class, resulting in a total of 1000 training points that were used for the classification.

After selecting the training points, we proceed to classification by instantiating a few classifiers including Random Forest, Classification and Regression Tree as well as Support Vector Machines, and training the classifier using the training data. In the following research study, we have discussed why we chose Random Forest as our algorithm to proceed with change detection over the other two classifiers. The results of the LULC for the year 2020 and 2021 at Wang Kelian district after the classifications by the Random Forest classifier has been presented in Figure 8 below.

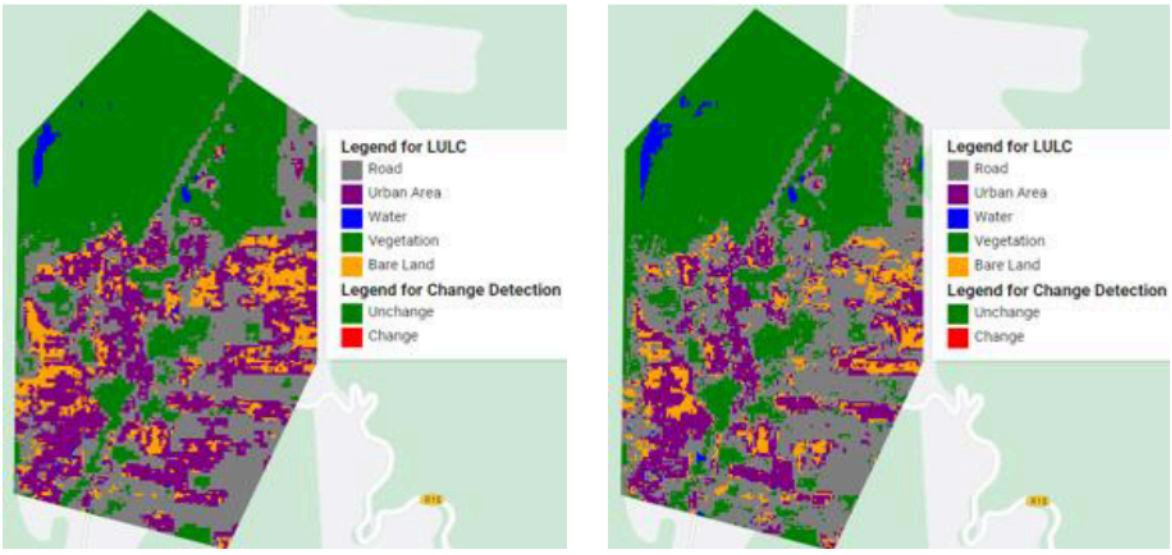

(a) (b)

Figure 8. LULC at Wang Kelian by using Random Forest classifier for year (a) 2020 (b) 2021

Obtaining a quantitative evaluation of the classifications' accuracy is critical. A common technique for accomplishing this is to divide the training samples into two random fractions, one for training the model and the other for validating the predictions. After training a few classifiers, they can be used to classify an entire image. The categorized values can then be compared to the validation fraction values. From the total 1000 training data points, we split it into a ratio of 70:30 where 70% of the data were used for training and 30% of the data were used for testing the three classifiers which are CART, Random Forest, and SVM. Each classifier has specific coding that needed to be implemented to obtain the classification result as mentioned in the methodology. The results of the confusion matrix and other assessments for the training and testing of the three classifiers can be seen from the Table 2, Table 3 and Table 4 below.

Table 2. Confusion matrix and accuracy assessment of 70% training and 30% test for Random Forest classifier

	Confusion Matrix of 70% Training Point (Random Forest)					Confusion Matrix of 30% Test Point (Random Forest)				
Class	(0)	(1)	(2)	(3)	(4)	(0)	(1)	(2)	(3)	(4)
Vegetation (0)	136	0	0	0	0	56	3	1	0	4
Road (1)	0	139	2	0	0	6	41	4	7	1
Urban Area (2)	0	0	142	0	0	1	10	43	2	0
Bare Land (3)	0	0	0	134	0	0	8	2	55	1
Water (4)	1	0	0	0	135	7	5	0	0	52
Overall Training Accuracy	0.995645864					0.799352751				
Overall Training Kappa	0.994556601					0.748951672				

Table 3. Confusion matrix and accuracy assessment of 70% training and 30% test for SVM classifier

	Confusion Matrix of 70% Training Point (SVM)					Confusion Matrix of 30% Test Point (SVM)				
Class	(0)	(1)	(2)	(3)	(4)	(0)	(1)	(2)	(3)	(4)
Vegetation (0)	124	0	1	0	10	60	0	0	0	5
Road (1)	28	105	8	2	1	15	34	6	1	0
Urban Area (2)	3	54	74	7	1	1	25	27	2	0
Bare Land (3)	12	29	25	69	3	4	9	11	36	2
Water (4)	19	15	0	0	100	11	3	1	1	50
Overall Training Accuracy	0.680115274					0.680921053				
Overall Training Kappa	0.599927292					0.600476913				

Table 4. Confusion matrix and accuracy assessment of 70% training and 30% test for CART classifier

	Confusion Matrix of 70% Training Point (CART)					Confusion Matrix of 30% Test Point (CART)				
Class	(0)	(1)	(2)	(3)	(4)	(0)	(1)	(2)	(3)	(4)
Vegetation (0)	144	0	0	0	0	39	5	2	0	10
Road (1)	0	149	0	0	0	2	36	7	4	2
Urban Area (2)	0	0	150	0	0	0	8	33	6	1
Bare Land (3)	0	0	0	142	0	0	5	5	44	4
Water (4)	0	0	0	0	136	4	5	0	3	52
Overall Training Accuracy	1					0.706462094				
Overall Training Kappa	1					0.669710235				

Based on the analysis of the classification results, it was determined that the Random Forest classifier is the most suitable for the study's purpose. This decision was made due to the high accuracy of the training and testing results, as well as the lack of overfitting. Other classifiers, such as CART and SVM, were found to have lower accuracy or overfitting issues. Additionally, the Naive Bayes classifier was determined to be insufficient for the study, as it produced unsatisfactory results. The Random Forest classifiers' training accuracy of 99.6% and testing accuracy of 80% indicate its reliability and trustworthiness for the classification process.

3.3 Change Detection

To analyse changes in land cover, we employed the technique of image subtraction on the LULC classifications obtained for two different time periods. This involved subtracting the values of each matched band in the LULC image from 2020 from the corresponding band in the LULC image from 2021, for all matched pairs of bands. Based on the change detection analysis by unsupervised classification of LULC, the total area changes were calculated to be 23.56 km² for Lahad Datu and 20.51 km² for Sungai Golok as seen from Figure 9 below. The change detection results of supervised classification were obtained for three locations: Wang Kelian, Sungai Golok and Pengerang, resulting in a total change of 94.74 km². Figure 10 and Figure 11 represent these results, demonstrating the outcome of LULC change detection using supervised classification.

(a) (b)

Figure 9. Result of change detection of unsupervised classification at (a) Lahad Datu (b) Sungai Golok

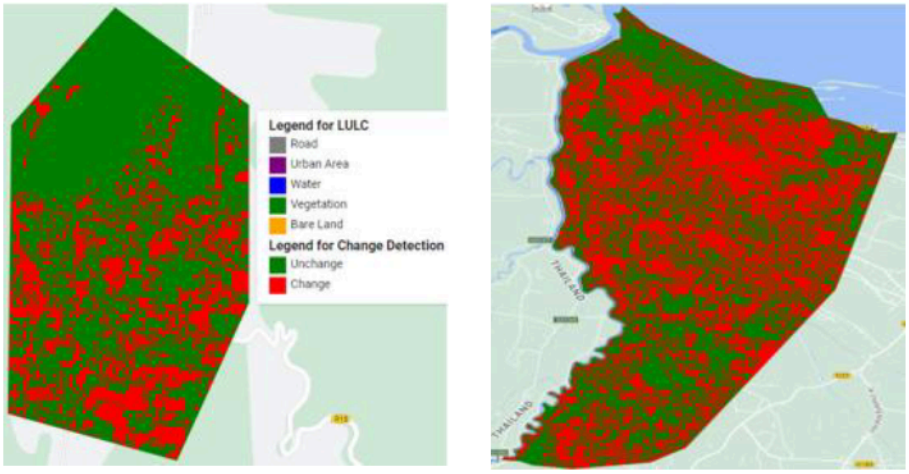

(a) (b)

Figure 10. Result of change detection of supervised classification at (a) Wang Kelian (b) Sungai Golok

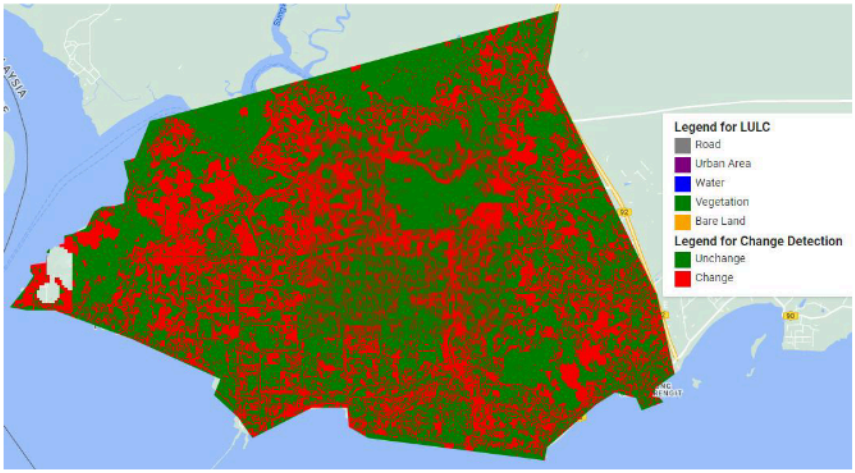

Figure 11. Result of change detection of supervised classification at Pengerang

4. CONCLUSION

This study demonstrates the effective application of machine learning methods, particularly the Random Forest classifier, for land use and land cover (LULC) classification and change detection using satellite imagery within the GEE environment. A key contribution of this work is the comparative evaluation of classical supervised classifiers, where Random Forest achieved the highest accuracy and showed robustness without overfitting. The implementation of K-means clustering for unsupervised classification also provides a useful baseline when labelled data is limited. However, the study has several limitations. The free version of GEE restricts processing power and storage, which constrained the size of training datasets and prevented the use of more complex models. Additionally, deep learning methods were not included in this study due to the platform's implementation limitations. Future work will aim to incorporate deep learning

models using external platforms and evaluate their performance against classical classifiers. Expanding the study to cover more diverse regions and larger datasets will further support the development of reliable, scalable tools for LULC monitoring in tropical and urban environments.

ACKNOWLEDGEMENTS

This research is supported by International Islamic University Malaysia under the KOE Engineering Merit Scholarships 2023 (KOEiems2023).

REFERENCES

[1] S. I. Hay, "An overview of remote sensing and geodesy for epidemiology and public health application," *Advances in Parasitology*, vol. 47, pp. 1–35, 2000.

[2] M. A. A. Asming, A. M. Ibrahim, and I. M. Abir, "Processing and classification of landsat and sentinel images for oil palm plantation detection," *Remote Sensing Applications: Society and Environment*, vol. 26, p. 100747, 2022.

[3] R. Congalton, "Remote sensing: An overview," *GIScience and Remote Sensing*, vol. 47, no. 4, pp. 443–459, 2010.

[4] J. Kurihara, Y. Takahashi, Y. Sakamoto, T. Kuwahara, and K. Yoshida, "HPT: A high spatial resolution multispectral sensor for microsatellite remote sensing," *Sensors (Switzerland)*, vol. 18, no. 2, 2018.

[5] X. Feng, L. He, Q. Cheng, X. Long, and Y. Yuan, "Hyperspectral and multispectral remote sensing image fusion based on endmember spatial information," *Remote Sensing*, vol. 12, no. 6, p. 1009, 2020.

[6] G. Crucil, F. Castaldi, E. Aldana-Jague, B. van Wesemael, A. Macdonald, and K. van Oost, "Assessing the performance of UAS-compatible multispectral and hyperspectral sensors for soil organic carbon prediction," *Sustainability*, vol. 11, no. 7, p. 1889, 2019.

[7] N. Davaasuren, J. Stapel, C. J. Smit, and N. Dankers, *The use of Remote sensing as a monitoring tool for coastal defence issues in the Wadden Sea*, No. C057/12. IMARES, 2012.

[8] A. B. Pour and M. Hashim, "Application of Landsat-8 and ALOS-2 data for structural and landslide hazard mapping in Kelantan, Malaysia," *Natural Hazards and Earth System Sciences*, vol. 17, no. 7, pp. 1285–1303, 2017.

[9] J. Théau, *Change Detection* (pp. 77–84). *What is Remote Sensing? The Definitive Guide - GIS Geography*. (n.d.). Retrieved January 16, 2023, from https://gisgeography.com/remote-sensing-earth-observation-guide/

[10] S. Sagnika, S. Bilgaiyan, S. Mishra, B. Shankar, and B. S. P. Mishra, "An exploration of change detection techniques for images," *Journal of Theoretical and Applied Information Technology*, vol. 64, no. 3, pp. 820-836, 2014.

[11] J. Wang and F. Biljecki, "Unsupervised machine learning in urban studies: A systematic review of applications," *Cities*, vol. 129, p. 103925, 2022.

[12] D. B. Thakkar, A. V. Patel, and M. Patel, "Geometric distortion and correction methods for finding key points: A survey," *International Journal for Scientific Research & Development*, vol. 4, no. 2, pp. 311-314, 2016.

[13] D. R. Panuju, D. J. Paull, and A. L. Griffin, "Change detection techniques based on multispectral images for investigating land cover dynamics," *Remote Sensing*, vol. 12, no. 11, p. 1781, 2020.

[14] S. Mishra, P. Shrivastava, and P. Dhurvey, "Change detection techniques in remote sensing: A review. *International Journal of Wireless and Mobile Communication for Industrial Systems*, vol. 4, no. 1, pp. 1–8, 2017.

[15] P. Lemenkova and O. Debeir, "R Libraries for remote sensing data classification by k-means clustering and NDVI computation in Congo River Basin, DRC," *Applied Sciences*, vol. 12, no. 24, p. 12554, 2022.